Apparent longitudinal relaxation of mobile spins in thin, periodically excited slices

Achim Gädke, Nikolaus Nestle

TU Darmstadt, Institute of condensed matter physics, Germany

Corresponding author:
Prof. Dr. Nikolaus Nestle
TUD, IFP
Hochschulstraße 6
D-64289 Darmstadt
E-Mail: nikolaus.nestle@physik.tu-darmstadt.de

Abstract

In this contribution, we present simulations and first experimental results on the apparent longitudinal relaxation behavior of mobile spins in thin periodically excited slices. This phenomenon is especially of interest in the context of NMR microimaging at extremely high spatial resolution and also for the development of mechanically detected NMR on biological samples under semiambient conditions. In the most simple case, the signal amplitude available in such an experiment is determined by the recovery of saturated in-slice magnetization during the time interval between two excitations. This magnetization recovery results both from relaxation and from diffusive exchange with magnetization outside the slice. We recently studied the combined effect of relaxation and diffusion in a simple saturation-recovery experiment on a fully relaxed sample. In the case of periodic excitation, the diffusion balance is complicated by the fact that there is also partially excited out-of-slice magnetization left over from earlier excitation cycles.

NMR, diffusion, relaxation, MRI, microimaging, Mechanically Detected Magnetic Resonance (MDMR), Magnetic Resonance Force Microscopy (MRFM)

1. Introduction

NMR experiments involving thin excited slices are of interest both for conventional NMR imaging and for mechanically detected magnetic resonance. Furthermore, thin excited slices are unavoidable in static ultra-high field gradient diffusometry experiments [1] where the excited slice of the sample is limited by the spectral bandwidth of the RF pulses. In NMR microimaging, several groups have recently reported slice thicknesses on the order of several µm both for standard MRI approaches [2] and for specialized techniques such as STRAFI [3] and SPI [4], and even much higher resolutions are considered feasible [5]. In mechanically detected NMR, the thickness of the excited slices will also be well below 1 µm, possibly even in the nm-range [6]. In samples containing fast-diffusing liquid components such as water, the diffusive exchange of spin magnetization between the excited slice and its surroundings on the time scale of the NMR experiments plays a major role. In a recent experiment [7], we have studied the

influence of the diffusion balance on the apparent longitudinal relaxation behaviour measured in a saturation-recovery experiment. The results of this study suggest that in a 1 µm slice with a Gaussian profile, the apparent longitudinal relaxation time of water may be as short as 0.87 ms.

Under the conditions of the experiment described above, the sample was allowed for full spin relaxation (with the well-known bulk relaxation time) between each run of the saturation-recover experiment. In an actual imaging experiment or even more so in mechanically detected NMR [6], we can expect much faster and periodic excitation cycles. Under these conditions, the diffusive magnetization balance between the excited slice and its surroundings needs considering excited magnetization from previous excitation cycles, too. In contrast to the single-excitation scenario described in [7], the periodic excitation scenario is not accessible to a simple analytical solution. Instead, we have modeled the magnetization balance numerically. After shortly reviewing the single-excitation experiment and describing the model for the multiple-excitation scenario under consideration here, we will describe some simulation results. After that some first experimental results will be described which were obtained using a new home-built spectrometer platform [8] allowing very flexible multitriggering.

2. Relaxation and diffusion balance in a thin excited slice

If a slice (thickness b) of an extended sample is excited in an NMR experiment, recovery of magnetization in the excited slice does not only occur due to relaxation but also due to diffusion. The relevant length scale for this diffusion effect is the saturation memory length l_{sm} which is given by the mean diffusive shift (orthogonal to the slice) of the excited molecules during the longitudinal relaxation time T_1:

$$l_{sm} = \sqrt{2DT_1} \quad (1)$$

Notable diffusion balance effects can therefore be expected in any situation where b is not $\gg l_{sm}$. The most simple experiment in which this balance effect can be studied is the saturation-recovery experiment: (excitation pulse with slice profile $P(x)$) – (variable time delay t) – (sampling pulse with slice profile $P(x)$) – (detection of signal $S(t)$).This experiment was used in [7]. In Fig. 1, the change of the excited slice profile due to diffusion is sketched. In the absence of diffusion effects, the magnetization $M(t)$ detected by the sampling pulse is given by

$$S(t) = M_o - \, <\Delta M(x,t)>_x \, = M_o(1 - Qe^{-t/T_1}) \quad (2)$$

with $Q = \, <P(x)P(x)>_x$ and $\Delta M(x,t)$ the local excited magnetization at time t.

In the presence of diffusive exchange with out-of-slice magnetization, Eq. 2 must be modified in order to take into account the diffusion balance. This results in

$$<M(t)>_x = M_o(1-QB(t)F(t)) \quad (3)$$

with $B(t) = \dfrac{<C(x,t)P(x)>_x}{<P(x)P(x)>_x}$ (4)

and $F(t)$ a purely time-dependent magnetization decay function.
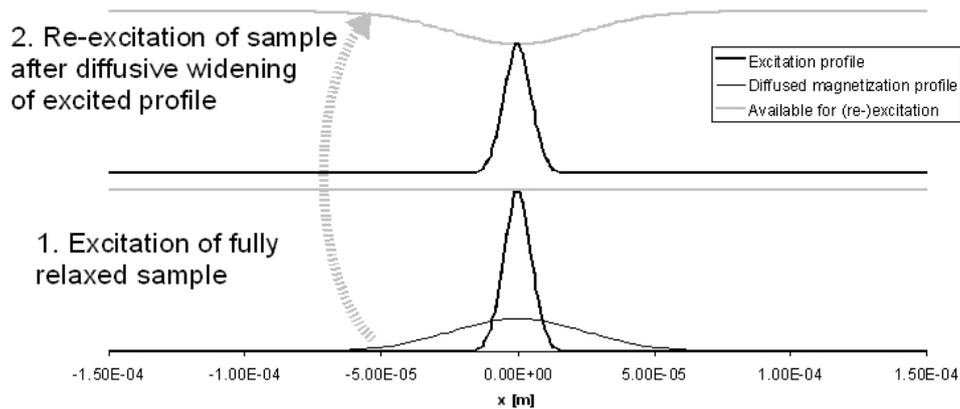
Fig. 1 Diffusive broadening of an excited magnezitation profile and resulting profile in a re-excitation after incomplete relaxation. The profiles in the figure represent the situation for a Gaussian excitation profile with an initial width of 5 µm and a re-excitation (or sampling) pulse with the same excitation profile applied after 100 ms. The diffusion coefficient is $3 \cdot 10^{-9}$ m^{2}s^{-1}. With a T_1 of 3 s, the magnetization losses due to relaxation during the diffusion time are still less than 4%.

The profile $C(x,t)$ is the solution of the diffusion equation

$$\frac{\partial C(x,t)}{\partial t} = D \frac{\partial^2 C(x,t)}{\partial x^2} \quad \text{with } C(x,t) = \Delta M(x,t)/M_o \text{ the initial condition } C(x,0) =$$

$P(x)$.

In [7], solutions for $B(t)$ are given for rectangular slice profiles and for Gaussian slice profiles. For the Gaussian profile, a simple expression for $B(t)$ can be derived:

$$B(t) = \frac{1}{\sqrt{1 + Dt/b^2}} \quad (5)$$

The resulting magnetization decay curve is plotted in Fig. 2 for two different slice thicknesses.

For $t << \dfrac{b^2}{D}$, the resulting magnetization decay curve can be approximated by a simple exponential decay with an apparent longitudinal relaxation time T_{1Diff} given by

$$\frac{1}{T_{1Diff}} = \frac{1}{T_1} + \frac{D}{2b^2} \quad (6)$$
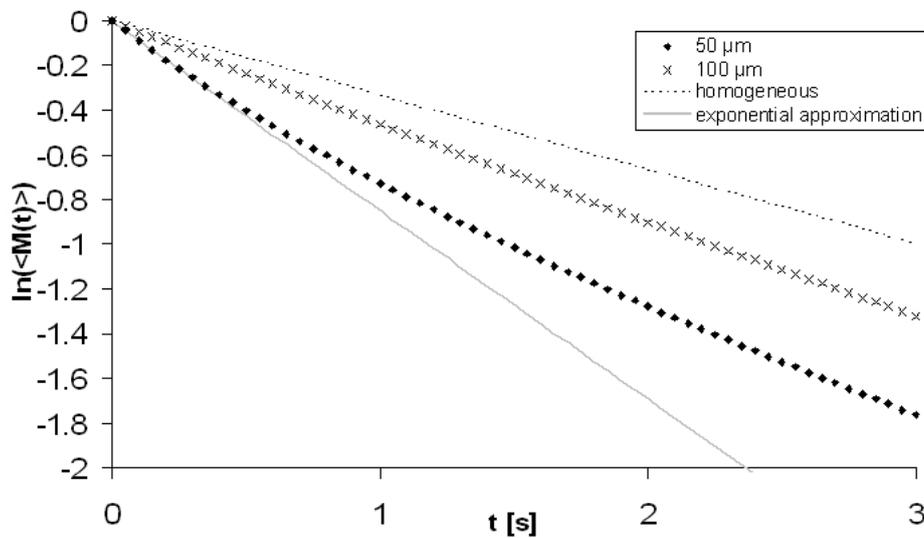
Fig. 2 Calculated magnetization decay curves for Gaussian excitation profiles of two different thicknesses and for a homogeneous sample. For the 50μm slice, also the exponential approximation of the initial magnetization decay with T_{1Diff} is shown. (Parameters: $D = 3·10^{-9}$ m²s⁻¹, $T_1 = 3$s).

For water ($T_1 = 3$s, $D = 2.3·10^{-9}$ m²s⁻¹) and a 1 μm Gaussian excited sample, Eq. 6 suggests a T_{1Diff} of 0.87 ms! As T_1 is both a limiting parameter for the signal accumulation and a contrast parameter in MRI experiments, such a dramatic reduction in the apparent T_1 might have dramatic consequences for MRI at microscopic resolution. However, in MRI (and even more in mechanically detected NMR), there is not just one but a periodic train of saturating pulses. At the time of the Nth saturating pulse, there will therefore be excited magnetization from all previous N-1 excitations outside of the excited slice. The presence of this magnetization (which experiences relaxation with the ordinary bulk T_1) reduces the influx of unsaturated magnetization into the excited slice. If the excitation is repeated with an excitation period $t_S << T_1$, the accumulation of excited magnetization outside the slice might eventually lead to a situation in which no notable influx of unsaturated magnetization into the slice occurs any more.

If we assume that the excitation occurs by means of instantaneous excitation pulses applied at times t_i and that there are no coherence effects, the diffusion balance of excited magnetization can be described by the following model:

$$\frac{\partial C(x,t)}{\partial t} = D\frac{\partial^2 C(x,t)}{\partial x^2} - \frac{C(x,t)}{T_1} + \sum_{t=1}^{N} M_o(1 - C(x,t))P(x)\delta(t - t_i) \quad (7)$$

For a periodic excitation, t_n is equal to nt_s, and we can write Eq. 7 as:

$$\frac{\partial C(x,t)}{\partial t} = D\frac{\partial^2 C(x,t)}{\partial x^2} - \frac{C(x,t)}{T_1} + \sum_{t=n}^{N} M_o(1 - C(x,t))P(x)\delta(t - nt_s) \quad (8)$$

Eq. 8 is dependent from three different length scales resp. time scales corresponding to length scales:

- The slice thickness b of the excited profile,
- The saturation memory length l_{sm} which was defined in Eq. 1 and
- The excitation mixing length l_{em} which corresponds to the mean diffusive shift of the molecules during the excitation period t_s: $l_{sm} = \sqrt{2Dt_s}$

Diffusion balance effects are irrelevant if $b \gg l_{sm}, l_{em}$. For $b \ll l_{em}$, the influence of magnetization left over from earlier excitation cycles becomes negligible and the magnetization decay behaviour approximates more and more that of the single excitation scenario. In a situation with $l_{sm} \gg b \approx l_{em}$, however, the effect of all three length scales must be taken into account and a numerical solution will be the method of choice.

3. Numerical solution of the multiple-excitation scenario

The solution is presently performed by means of a simple Gauss approach. The 1D sample space is discretized into typically about 2000 volume elements with a thickness Δx of 0.2 µm. For the time step Δt, a value of 1 µs is used. These values fulfill the condition $\frac{D\Delta t}{(\Delta x)^2} < \frac{1}{2}$ which must be met for a numerically stable solution of the diffusion equation. With typical values of $T_1 = 3$s, $D = 3 \cdot 10^{-9}$ m^{2}s^{-1} and t_s on the order of 1 ms, the magnetization balance is simulated over a time window of several seconds. This takes about 10 min on a PC equipped with an intel 1.6 GHz Pentium processor. The simulation procedure is summarized in Fig. 3. It is presently implemented into a Free Pascal program [9].

Two types of visualizations of the simulation outcome are available at the moment: the amplitude of the excitable in-slice magnetization

$$M_E(t) = \int (M_o - \Delta M(x,t))P(x)dx \quad (9)$$

and the overall inventory of excited magnetization

$$I_{Mag}(t) = \int \Delta M(x,t)dx \quad (10)$$

are computed as a function of time (see Fig. 4), and the time development of the spatial distribution of excited magnetization is visualized in a spatiotemporal greyshade plot (see Fig. 5).

1 Diffusion:

$$\tilde{c}_i(t+\Delta t)=c_i(t)+\frac{D\,\Delta t}{(\Delta x)^2}(c_{i+1}(t)+c_{i-1}(t)-2\,c_i(t))$$

2 Relaxation

$$c_i(t+\Delta t)=\tilde{c}_i(t+\Delta t)-\frac{\tilde{c}_i(t+\Delta t)}{T_1}$$

$$t<nt_s\leq t+\Delta t\ ?$$

no

$$t=t+\Delta t$$

$$n=n+1$$

yes

$$c_i(t)=c_i(t)+(M_o-c_i(t))P(x,b)$$
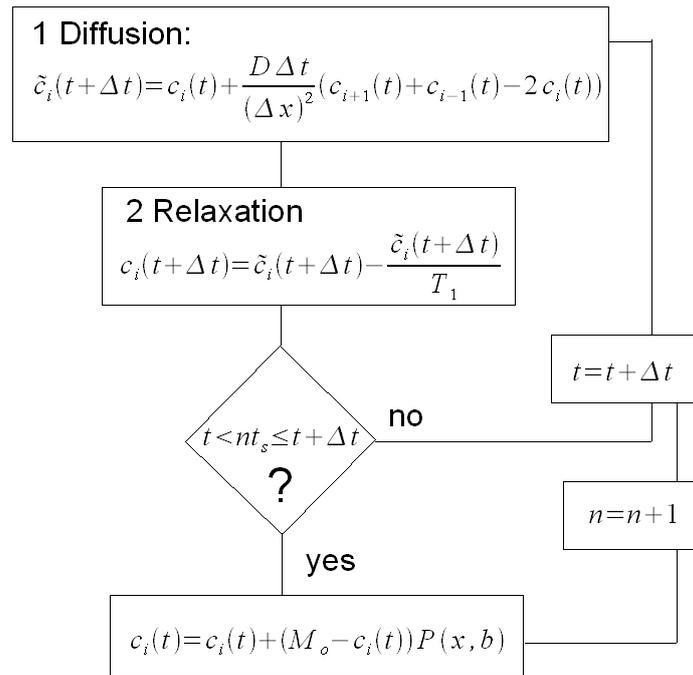
Fig. 3 Flow chart summary of the main steps of the simulation routine.
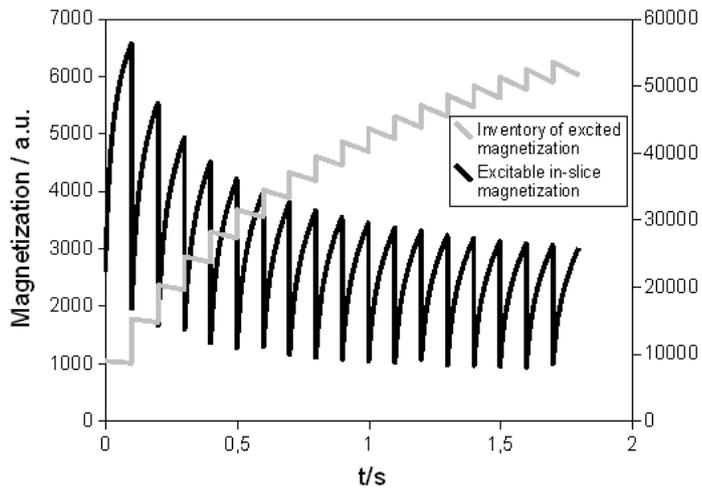
Fig. 4 Simulated development of excitable in-slice magnetization in a 10 μm Gaussian slice and the overall inventory of excited magnetization in a sample with D = 3·10^{-9} m^{2}s^{-1}, T_1 = 3s and with t_s = 0.1 s.
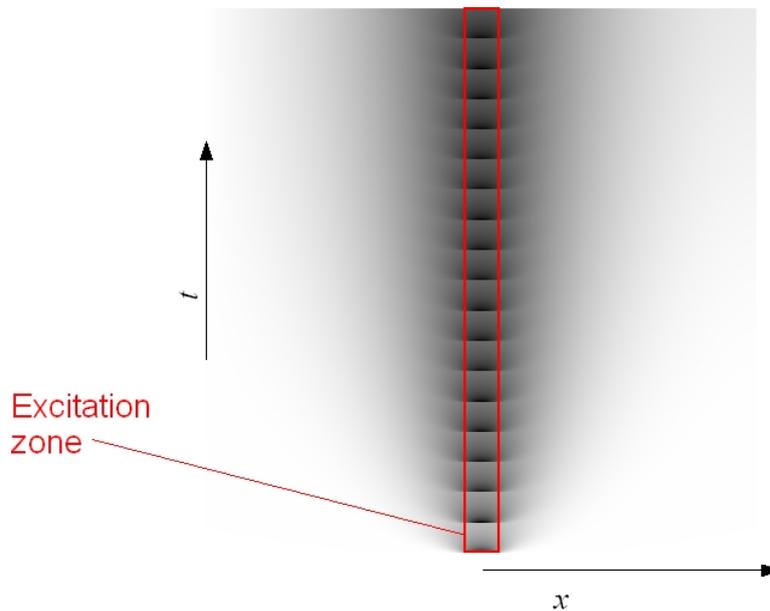
Fig. 5 Representation of the same simulation run as in figure 4 in a spatiotemporal grayshade plot (fully saturated magnetization: black, equilibrium magnetization: white). Note the long-range spread of out-of-slice magnetization following a square root of time law typical for diffusive processes.

4. Simulation results and scale analysis

In Fig. 6, the simulated NMR signal amplitude after each excitation event is plotted as a function of time for several different values of the slice thickness b. In Fig. 6A, the absolute modulation amplitudes are plotted, in Fig. 6B, the modulation amplitudes are plotted relative to the signal amplitude in the first excitation cycle. As one can see from the figure, the signal amplitude decreases during the first excitation cycles and slowly tends to a steady state. The amplitude in the steady state relative to the initial signal amplitude becomes lower with increasing slice thickness. Also, the number of excitation cycles it takes to reach the steady state is smaller for thick excited slices compared to thinner slices.

The initial signal intensity in the thicker slices is higher than in the thinner slices as there is much more excitable material in the thick slices. Furthermore, the steady state signal in the thick slice also contains a contribution from relaxation inside the slice. In order to quantify the contribution of the diffusion balance effect to the overall signal it is therefore of interest to compare the simulated signal amplitudes with the signal amplitude that can be expected on the basis of in-slice relaxation alone. Like this, the relative signal enhancement E_{Diff} by the diffusion balance effect results as:

$$E_{Diff} = \frac{\int (M_o - \Delta M(x, nt_s)) P(x) dx}{M_o Q e^{-\frac{t_s}{T_1}}} \quad (11)$$
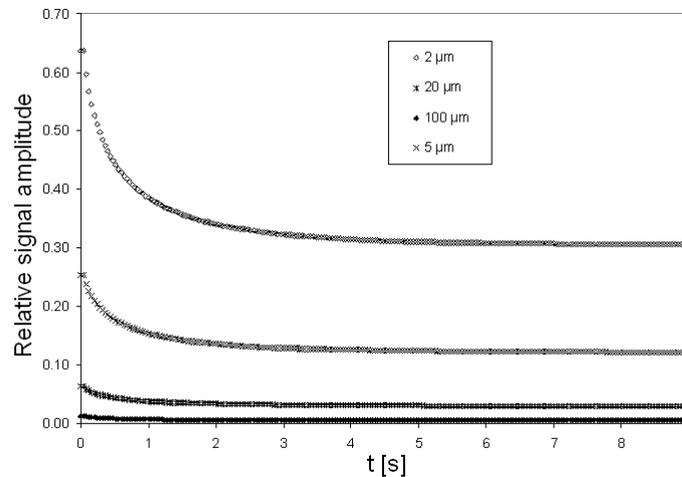
Fig. 6 Simulated NMR signal amplitude in successive excitation events computed for $T_1 = 3s$, $D = 3 \cdot 10^{-9}$ m^{2}s^{-1}, $t_s = 40$ ms and various slice thicknesses. A: absolute signal amplitudes, B: relative signal amplitude normalized to the intensity in the excitation of the fully relaxed sample.

It is of interest to study also the dependence of the NMR signal amplitude on sample properties such as the self-diffusion coefficient and the longitudinal relaxation time. In this case, it is possible to compare the absolute signal amplitudes with each other as no

change in the thickness of the excited slice takes place. Fig. 7 A shows simulation results for variations of the self-diffusion coefficient D, Fig. 7 B for the variation of the longitudinal relaxation time T_1. In both cases, t_s was chosen so short that in-slice-relaxation did not play a significant role for the observable NMR signal amplitude.
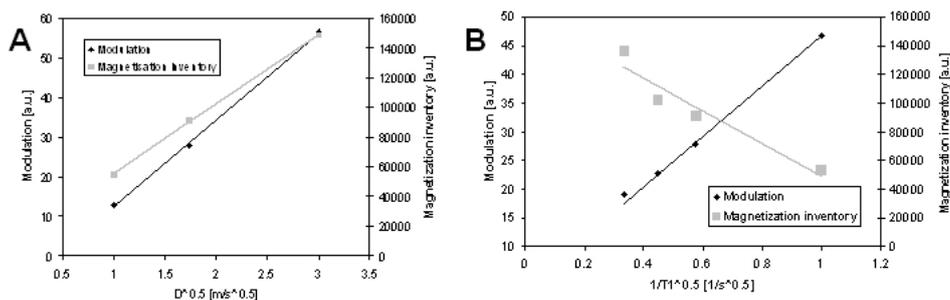
Fig. 7 Dependence of the steady state signal intensity achieved in a periodically excited slice on the self-diffusion coefficient and on the longitudinal relaxation time. Parameter variations in the simulation were conducted using the following set of parameters as a starting point: for $T_1 = 3$s, $D = 3 \cdot 10^{-9}$ m^{2}s^{-1}, $t_s = 2$ ms, $b = 2$ μm.

As one can see from the figures, the signal amplitude in the steady state increases proportional to the square root of the diffusion coefficient and inversely proportional to the longitudinal relaxation time. Both these findings can be understood by means of a simple scale analysis: The outflow of excited magnetization from the slice during the excitation period t_s is proportional to the diffusive flow from the slice to the surroundings. The diffusive flow responsible for transport of unsaturated magnetization into the slice must occur over a the length scale of the saturation memory length and is proportional to the self diffusion coefficient:

$$ j_{Diff} \propto \frac{D}{\sqrt{2DT_1}} = \sqrt{\frac{D}{2T_1}} \quad (12) $$

5. New spectrometer platform and first experimental results

The selective NMR excitation of a very thin slice is most easily realized in the presence of a magnetic field gradient. In standard clinical MRI, slices with a thickness on the range of several mm are excited in the presence of magnetic field gradients on the order of 10 mT/m. The duration of the corresponding narrow-band RF pulses is typically several 100 μs. In a stronger gradient of several 10 T/m such as it can be found in the fringe field of a superconducting NMR magnet or in the even higher gradients that are available in dedicated gradient NMR magnets [1], even a short, broad-band RF pulse of a duration of several μs will unwantedly lead to a slice-selective excitation [10]. When a pulse with the same spin flip angle but longer duration (i.e. with a reduced RF power) is irradiated, the excitation bandwidth of this pulse is smaller than for a short RF pulse due to its reduced frequency bandwidth. Reducing the pulse power by about 40 dB will therefore allow the excitation of very thin sample slices with a thickness of just a few μm

[7]. In the present work, slice thicknesses on the order of a few μm could be reached for excitation pulses of 35 μs duration in the presence of a static magnetic field gradient of 180 T/m. Under such field conditions, it is not possible to detect an FID of the sample ($T_2^* < 2$ μs). Therefore, the excitable magnetization cannot be detected by measuring the FID amplitude but an echo has to be used instead. In order for the echo to be representative for the magnetization in the excited slice, one has to make sure the echo is generated from the same slice as the excited magnetization. This won't be the case for a 180° pulse realized by doubling the pulse duration compared to the 90° pulse: the longer 180° pulse will exhibit a smaller excitation bandwidth than the 90° pulse. In order to present this problem, we have chosen to use identical pulses for excitation and generation of the echo (see Fig. 8).
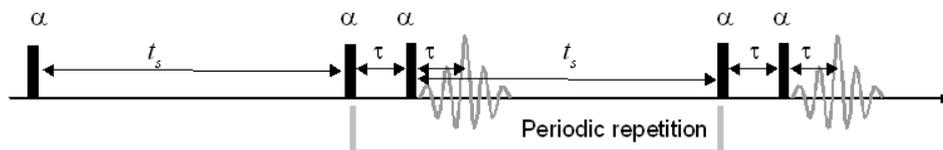
Fig. 8 Pulse sequence used for studying the periodic modulation of a thin excited slice of magnetization in a magnet with a large static gradient field in which the longitudinal magnetization cannot be probed with an FID. As t_s is much longer than the echo duration, the signal acquisition is limited to the actual echo time, so than multitriggering is needed for the experiment.

This type of echo is called a "eight ball" echo in the literature and behaves essentially like a spin echo except for its amplitude which is only half that of the spin echo [11]. In a strong magnetic field gradient, the echo intensity is reduced not only due to transverse relaxation but also due to diffusion effects. This reduction only is during the time interval 2τ between RF pulse used for sampling the magnetization and the acquisition of the echo. The signal loss during this period is not dependent on the variable time delay t_s between the last exciting pulse and the sampling pulse. Therefore, the amplitude of the echo is directly proportional to the unsaturated magnetization available at the time of the sampling pulse. A similar pulse sequence was used in the experiments reported in [7]. The only difference now is that now there is a whole train of t_s-90°-τ-90°- echo-readout cycles applied now to the sample. As the time delay t_s is orders of magnitude longer than the echo duration (approximately $1/T_2^*$), this sequence can only be used on a spectrometer with multitriggering capabilities (see Fig. 8). These capabilities are provided by the new home-built open source spectrometer control platform DArmstadt MAgnetic Resonance Interface System (DAMARIS) which is presently under development at our institute [8]. This software is now also used at the original gradient magnet setup [1].
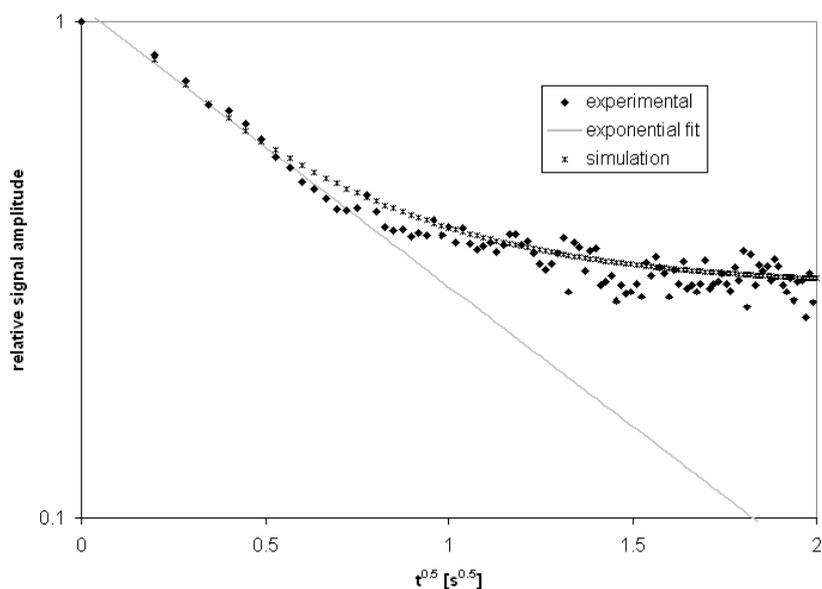
Fig. 9 Signal intensities experimentally recorded for a 3.2 μm slice in a water sample at room temperature (1000 accumulations), simulation (with $T_1 = 3s$, $D = 2.3·10^{-9}$ m^2s^{-1}, $t_s = 40$ ms) and exponential fit plotted in a semilogarithmic scale over the square root of modulation cycle duration.

As a running prototype of DAMARIS has become available only quite recently, we can only report first results from measurements using the sequence depicted in Fig. 8. In figure 9, the relative NMR signal intensity is shown as a function of the square root of the running time of the pulse train. As can be seen from the figure, the simulation and the experimental data correspond quite nicely to each other. Furthemore, the initial signal amplitudes decay linearly with the square root of time. This again can be understood in a scale analysis similar to the one discussed in Eq. 12: The mean diffusive shift of the excited magnetization from the slice increases with the square root of time. As the mean diffusive shift also corresponds to the length scale responsible for the diffusive flow of excited magnetization from the slice to the outer parts of the sample, the diffusive flow of unsaturated water into the excited slice decreased proportional to this length scale as long as magnetization losses due to out-of-slice relaxation can be neglected.

6. Conclusion and Outlook

Diffusion balance effects lead to changes in the apparent longitudinal relaxation behavior in thin excited slices. In a single-excitation scenario, the diffusion effect may lead to an apparent longitudinal relaxation time which is orders of magnitude shorter than the bulk value. In a situation with periodic excitation and an excitation period $t_s << T_1$, the diffusion balance effect in the steady state is much smaller than in the single-excitation case due to partially saturated out-of-slice magnetization left over from earlier

excitation cycles which reduces the diffusive flux of unsaturated magnetization into the excited slice.

The results presented here correspond to the state of the work at the time of the Diffusion Fundamentals Conference in Leipzig 2005. Further research is under way which covers the following aspects:

- Effects of out-of-slice diffusion barriers and relaxation sinks onto the diffusion balance effect in periodically modulated magnetizations. Such effects may play a decisive role in the development of novel contrast mechanisms for NMR microscopy and mechanically detected NMR imaging (MRFM). A similar idea called DESIRE suggested for contrast enhancement in MRI by the Lauterbur group in the early 90s [12] was recently successfully realized [13].
- Improvements in the simulation procedures by working with a variable discretization of the spatial dimension.
- Signal/Noise improvements in the experimental setup by further optimizing the coil design.

References

[1] I. Chang, F. Fujara, B. Geil, G. Hinze, H. Sillescu, A. Tölle, J. Non-Cryst. Sol. 172-174, (1994) 674-681.

[2] L. Ciobanu, A. G. Webb, C. H. Pennington, Progr. NMR Spectr. 42 (2003) 69–93

[3] G. Bennett, J.-P. Gorce, J. L. Keddie, P. J. McDonald, H. Berglind, Magn. Res. Imag. 21 (2003) 235–241.

[4] A. V. Ouriadov, R. P. MacGregor, B. J. Balcom, J. Mag. Res. 169 (2004) 174–186.

[5] J. H. Baltisberger, S. Hediger, L. Emsley, J. Mag. Res. 172 (2005) 79–84.

[6] N. Nestle, A. Schaff, W.S. Veeman, Progr. NMR Spectr. 38 (2001) 1-35.

[7] N. Nestle, B. Walaszek, M. Nolte, J. Mag. Res. 168 (2004) 46-52.

[8] A. Gädke, C. Schmitt, N. Nestle N, GDCh Magnetic Resonance discussion meeting, Mainz, Germany 26.-29.9.2005 XXX

[9] www.freepascal.org

[10] B. Geil, Concepts Magn. Res. 10 (1998) 299-321.

[11] M.T. Vlaardingerbroek, J.A. den Boer JA, Magnetic Resonance Imaging. Theory and Practice. Springer, Heidelberg, 1999.

[12] P. C. Lauterbur, W. B. Hyslop, H. D. Morris, XI International Society of Magnetic Resonance Conference, 1992, Vancouver, BC.

[13] L. Ciobanu, A.G. Webb , C. H. Pennington, J. Magn. Res. 170 (2004) 252–256.